
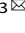


ARTICLE



Long non-coding RNA DLGAP1-AS1 modulates the development of non-small-cell lung cancer via the microRNA-193a-5p/DTL axis

Xudong Pan^{1,4}, Siwen Chen^{1,4}, Lu Ye¹, Shenjie Xu¹, Ling Wang^{1,2}  and Yi Sun³ 

© The Author(s), under exclusive licence to United States and Canadian Academy of Pathology 2022

Non-small cell lung cancer (NSCLC) is one of the most malignant cancers worldwide. A growing number of studies have suggested that long noncoding RNAs (lncRNAs) play a key role in the progression of non-small cell lung cancer (NSCLC). Here, we report a novel lncRNA DLGAP1 antisense RNA 1 (DLGAP1-AS1) that exhibits oncogenic properties in NSCLC. The lncRNA DLGAP1-AS1 and denticleless protein homolog (DTL) presented upregulated expression, but microRNA-193a-5p (miR-193a-5p) showed downregulated expression in cancerous tissues of human lung samples from 48 patients with NSCLC. Partial loss of lncRNA DLGAP1-AS1 reduced malignant cell viability, migration, and invasion but induced apoptosis. Dual-luciferase reporter gene, RNA pull-down and RNA binding protein immunoprecipitation assays demonstrated enrichment of lncRNA DLGAP1-AS1 in miR-193a-5p and Argonaute 2, suggesting that lncRNA DLGAP1-AS1 modulated DTL, a putative target of miR-193a-5p. We also found that restoration of miR-193a-5p rescued NSCLC cell biological functions affected by overexpression of lncRNA DLGAP1-AS1. Silencing lncRNA DLGAP1-AS1 was found to reduce the tumorigenesis of NSCLC cells xenografted into nude mice, which was rescued by DTL overexpression. In conclusion, our study highlights a novel regulatory network of the lncRNA DLGAP1-AS1/miR-193a-5p/DTL axis in NSCLC, providing a potential therapeutic strategy for NSCLC.

Laboratory Investigation (2022) 102:1182–1191; <https://doi.org/10.1038/s41374-022-00831-6>

INTRODUCTION

Lung cancer is the second most frequently occurring cancer and causes the most cancer-related deaths worldwide¹. Traditionally, there are two types of lung cancers according to histological variation: small cell lung cancer and non-small cell lung cancer (NSCLC). NSCLC accounts for approximately 85% of lung cancers and consists of three subtypes: squamous-cell carcinoma, large-cell carcinoma, and adenocarcinoma¹. Smoking is the top environmental risk factor that causes lung cancer. Patients with NSCLC who have a long history of smoking always suffer rapid disease progression and worse clinical outcomes². The symptoms in the early stage of NSCLC usually include short breath and continuous cough, possibly with blood sputum and chest pain. However, when NSCLC cells spread to distant tissues in late stages, complicated symptoms and failure of organ functions will present. Moreover, the 5-year survival rate of patients with NSCLC is only 15%, and patients usually die within half a year². Therefore, it is urgent to diagnose NSCLC in the early stage via effective means, such as the detection of early-diagnosed biomarkers. For example, epidermal growth factor receptor (EGFR) is identified as a common biomarker in the clinical diagnosis of NSCLC according to multiple studies on the genetics of NSCLC³. However, it was recently determined that EGFR mutations comprise only one-sixth of adenocarcinomas and one subtype of NSCLC. In addition, the

remaining genetic alterations exist in KRAS, multiple kinases and other unknown genes⁴. This heterogeneity results in drug resistance and recurrences after surgical resection, which hinder radical cure of NSCLC.

In recent years, deep sequencing has uncovered the important roles of noncoding RNAs, including long noncoding RNAs (lncRNAs) and microRNAs (miRNAs or miRs), in NSCLC. On the one hand, miRNAs are short single RNAs that usually control gene expression by regulating transcription and translation⁵. It has been shown that genome-wide research can produce the expression profile of serum miRNAs, which can then be used to predict the survival of patients with NSCLC⁶. The let-7 miRNA family has been proven to suppress tumor development in NSCLC⁷. Similarly, miR-193a-5p, which we discussed in this study, has been demonstrated to contribute to the metastasis of NSCLC⁸. On the other hand, lncRNAs are long functional transcripts over 200 nt in length that regulate cellular physiology and disease progression. Large numbers of lncRNAs, such as metastasis associated with lung adenocarcinoma transcript 1, HOX transcript antisense RNA and nuclear paraspeckle assembly transcript 1, have been identified to promote the proliferation and migration of NSCLC cells^{9,10}. Although lncRNA DLGAP1 antisense RNA 1 (DLGAP1-AS1) has not been investigated in the context of NSCLC, one report has suggested that it can exacerbate the aggressive behavior of

¹Department of General Medicine, The First Affiliated Hospital of Soochow University, Suzhou 215006, PR China. ²Department of General Medicine, Dushu Lake Hospital Affiliated to Soochow University, Suzhou 215000, PR China. ³School of Biology & Basic Medical Sciences, Suzhou Medical College of Soochow University, Suzhou 215123, PR China. ⁴These authors contributed equally: Xudong Pan, Siwen Chen. ✉email: wangling40@126.com; syixz524@suda.edu.cn

Received: 22 April 2021 Revised: 23 August 2021 Accepted: 15 October 2021

Published online: 1 October 2022

gastric cancer¹¹. In the present research, we first investigated the association of lncRNA DLGAP1-AS1 and miR-193a-5p in NSCLC. We found that lncRNA DLGAP1-AS1 interacted with miR-193a-5p, which specifically targeted denticleless protein homolog (DTL). Silencing lncRNA DLGAP1-AS1 or restoration of miR-193a-5p suppressed tumorigenesis of NSCLC.

MATERIALS AND METHODS

Bioinformatics analysis

Differential analysis was conducted with the gene expression dataset GSE19188 (including 91 NSCLC samples and 65 normal samples) and miRNA dataset GSE102286 (including 91 NSCLC samples and 88 normal samples) deposited in the Gene Expression Omnibus (GEO) database (<http://www.ncbi.nlm.nih.gov/geo/>). Briefly, the R language Affy package¹² was adopted to normalize the expression data, and the limma package¹³ was used for differential expression screening with the criterion $p < 0.05$. After identifying differentially expressed lncRNAs from the datasets GSE50627 (9 NSCLC cells and 6 normal cells) and GSE143018 (370 NSCLC tissues and 198 normal tissues), the LncAtlas (<http://lncatlas.crg.eu/>) database was employed to determine the subcellular location of lncRNAs and the expression of differentially expressed lncRNAs in the cytoplasm. Thereafter, miRNAs with possible binding sites to lncRNAs were predicted by the RNA22 database (<https://cm.jefferson.edu/ra22/>), and the results were intersected with differentially expressed miRNAs. mirDIP (<http://ophid.utoronto.ca/mirDIP/>), RNA22, TargetScan (http://www.targetscan.org/vert_71/), and miRWalk (<http://mirwalk.umm.uni-heidelberg.de/>) were adopted to predict the target genes of differentially expressed miRNAs, and the results were further intersected with the results of differentially expressed genes. Finally, Jvenn (<http://jvenn.toulouse.inra.fr/app/example.html>) was employed to compare the differences among various datasets, and a Venn diagram was plotted.

Clinical sample collection

A total of 48 surgically resected NSCLC tissues and adjacent normal tissues (located more than 5 cm away from the tumor) were collected from patients at The First Affiliated Hospital of Soochow University between 2013 and 2014¹⁴. Prior to sample collection, none of the patients received either local or systemic treatment. After collection, the tissue samples were placed in liquid nitrogen. Tissue type and tumor node metastasis were classified according to the National Comprehensive Cancer Network¹⁵.

Immunohistochemistry

The stored NSCLC tissues and adjacent normal tissues were embedded in paraffin and sectioned continuously at a thickness of 5 μ m. Next, rabbit polyclonal antibody to DTL (ab72264, 1:300, Abcam Inc., Cambridge, UK) was added to the sections and incubated at 4 °C overnight. Thereafter, the sections were incubated with biotin-labeled goat anti-rabbit immunoglobulin G (IgG) secondary antibody diluted at a ratio of 1:500 for 20 min at 37 °C. After staining with diaminobenzidine and counterstaining with hematoxylin, dehydration and transparency, the sections were observed under a microscope. Phosphate-buffered saline (PBS) was used as a negative control (NC) instead of primary antibody. The criterion for the staining results was as follows: protein expression was achieved by randomly selecting 5 tumor regions under a microscope. Positive cells were assigned percentages: 0 = 0%, 1 = 1%–10%, 2 = 11%–50%, 3 = 51%–70%, 4 = \geq 71%. Staining was ranked by intensity: 0 = no staining, 1 = weak staining, 2 moderate staining, and 3 = intense staining. Finally, DTL expression was assayed by the sum of the percentage of positive cells and the intensity of staining. After strict statistical analysis, the expression of DTL was divided into two stages: negative < 4 and positive ≥ 4 . Two pathologists blindly analyzed any discrepancies to avoid bias.

Cell culture

Five human NSCLC cell lines, A549, NCI-H1299, NCI-H1975, NCI-H358, and SK-MES-1, and the human bronchial epithelial cell line HBE (the cell bank of the Chinese Academy of Sciences: <http://www.cellbank.org.cn>) were cultured with Dulbecco's modified Eagle's medium (DMEM) (12800017, Gibco, Carlsbad, CA, USA) containing 10% fetal bovine serum (FBS, 26140079, Gibco) in an incubator (BB15, Thermo Fisher Scientific, Rockford, IL, USA) at 37 °C with 5% CO₂ under saturated humidity. The culture medium was renewed every 24 h. Cells were passaged every 72 h

and detached by 0.25% trypsin for 3 min. Detachment was terminated by adding DMEM supplemented with 10% FBS. Cells were converted to a single-cell suspension using a pipette, followed by conventional passage.

Cell treatment

The cells at logarithmic growth phase were infected with lentivirus and cultured for approximately 24 h. The culture continued for another 7 days in culture medium containing 1 μ g/mL puromycin to screen out stably infected cells. Reverse transcription quantitative polymerase chain reaction (RT-qPCR) and Western blot analysis were employed to assess the expression of the target genes. The three interference short hairpin (sh)-RNA sequences of lncRNA DLGAP1-AS1 were as follows: The sequences for shRNA-1 against DLGAP1-AS1 (sh-DLGAP1-AS1-1) were 5'-AGAGCUU-GAAACCUACCAA-3' (sense) and 5'-UUGGUAGUUUCAAGCUCU-3' (antisense), sh-DLGAP1-AS1-3': 5'-GAGCUUGAAACCUACCAAG-3' (sense) and 5'-CUUGGUAGUUUCAAGCUC-3' (antisense), sh-DLGAP1-AS1-3: 5'-AGAA-GUCCAACAUCGCAA-3' (sense), and 5'-UUGCGAUGUUGGAACUUCU-3' (antisense).

Cells were inoculated into 6-well plates 24 h before transfection. Next, the cells were transfected with the plasmids sh-DLGAP1-AS1, pcDNA-DLGAP1-AS1, miR-193a-5p mimic, pcDNA-DLGAP1-AS1 + miR-193a-5p mimic, sh-DLGAP1-AS1 + pcDNA-DTL, pcDNA-DTL and their corresponding controls using Lipofectamine 2000 (11668019, Thermo Fisher Scientific) per the manufacturer's instructions. All plasmids and vectors were constructed, sequenced, and identified, and virus packaging and titer detection were conducted by Shanghai Genechem Co., Ltd. (Shanghai, China).

RNA extraction and quantification

Total RNA was extracted from cells and tissues using TRIzol reagent (Invitrogen, Carlsbad, CA, USA). Next, the extracted RNA was reverse transcribed into complementary DNA (cDNA) in accordance with the instructions of both the PrimeScript RT kit (TaKaRa, Japan) and the cDNA RT kit (K1622, Beijing Yaanda Biotechnology Co., Ltd., Beijing, China). Thereafter, RT-qPCR was performed with the use of an ABI 7500 real-time PCR system (Life Technologies Corporation Gaithersburg, MD, USA) and a SYBR[®] Premix Ex Taq[™] II kit (TaKaRa). U6 was employed as an internal reference for miR-193a-5p and glyceraldehyde-3-phosphate dehydrogenase (GAPDH) for lncRNA DLGAP1-AS1 and DTL, with the primer sequences listed in Table S1. The fold changes between the experimental group and the control group were calculated by means of relative quantification ($2^{-\Delta\Delta C_t}$ method).

Western blot analysis

The total protein of tissues and cells was extracted with the use of precooled radioimmunoprecipitation assay lysis buffer (R0010, Beijing Solarbio Science & Technology Co., Ltd., Beijing, China) containing phenylmethylsulfonyl fluoride at 4 °C. The total extracted protein was subsequently quantified using a bicinchoninic acid protein assay kit (20201E576, YEASEN Biotechnology Co., Ltd., Shanghai, China) and thereafter separated by sodium dodecyl sulfate-polyacrylamide gel electrophoresis, after which the extracted protein was transferred onto polyvinylidene fluoride membranes with a wet transfer method. The membrane subsequently underwent blockade with 5% bovine serum albumin (BSA) at room temperature for 1 h and then was incubated at 4 °C with the addition of primary rabbit polyclonal antibody to DTL (1:5000, ab72264, Abcam Inc., Cambridge, UK) overnight. After 3 washes using Tris-buffered saline Tween-20 (TBST) (10 min/wash), the membranes were incubated with the addition of horseradish peroxidase-conjugated secondary antibody IgG (1:5000, 10494-1-AP, ProteinTech Group, Chicago, IL, USA) at room temperature for 1 h. After an additional 3 washes using TBST (10 min/wash), the membranes were developed using developer solution. Finally, the band intensities were quantified using Quantity One v4.6.2 software. The ratio of the gray value of the target band to GAPDH was representative of the relative protein expression.

Dual luciferase reporter gene assay

The wild-type (Wt) and mutant (Mut) sequences of lncRNA DLGAP1-AS1 and the DTL 3'-untranslated region (3'UTR) were artificially synthesized. Then, pmiR-RB-REPORT[™] plasmids (Guangzhou RiboBio Co., Ltd., Guangzhou, Guangdong, China) underwent enzyme digestion *via* restriction endonuclease. Next, the artificially synthesized Wt and Mut fragments were introduced into the pmiR-RB-REPORT[™] vectors (RiboBio). Meanwhile, empty plasmids were transfected as the control. Next, the correctly

sequenced luciferase reporter plasmids Wt and Mut were cotransfected with NC mimic or miR-193a-5p mimic into HEK-293T cells. After a 48 h period of transfection, the cells were collected and lysed, followed by centrifugation for 3–5 min and the collection of supernatant. The relative luciferase activity (RLU) was detected using a luciferase assay detection kit (RG005, Beyotime Institute of Biotechnology, Shanghai, China) with firefly luciferase taken as an internal reference. The RLU was expressed as the ratio of the RLU value of firefly luciferase to the RLU value of Renilla luciferase.

RNA pull-down assay

Cells were transfected using 50 nM biotin-labeled Bio-miR-193a-5p-Wt and Bio-miR-193a-5p-Mut (Wuhan GeneCreate Biological Engineering Co., Ltd., Wuhan, China). After 48 h, the cells were harvested and rinsed using PBS. Next, the cells were incubated for 10 min in specific lysis buffer (Ambion, Austin, Texas, USA). The lysate was incubated at 4 °C with M-280 streptavidin magnetic beads (S3762, Sigma-Aldrich Chemical Co., St Louis, MO, USA) precoated with RNase-free BSA and yeast tRNA (TRNABAK-RO, Sigma-Aldrich) overnight. For the next step, the aforementioned cell lysate and the magnetic beads were washed twice with precooled lysis buffer, three times with low salt buffer and once with high salt buffer. The bound RNA was purified using TRIzol, and lncRNA DLGAP1-AS1 enrichment was examined by RT-qPCR.

RNA binding protein immunoprecipitation (RIP)

Binding analysis of lncRNA DLGAP1-AS1, miR-193a-5p and Argonaute 2 (Ago2) was conducted according to the instructions of the RIP kit (Millipore, Billerica, MA, USA). In short, the cells were washed using precooled PBS, and the supernatant was discarded. The cells were then lysed on ice for 30 min using lysis buffer of equal volume containing ribonuclease inhibitor and protease inhibitor, followed by centrifugation at 14000 rpm at 4 °C for 10 min, with the supernatant obtained. Next, a portion of the cell extract was removed as input, and a portion was incubated with antibody for coprecipitation. In brief, 50 μ L of magnetic beads for each coprecipitation reaction system was extracted, washed, and then resuspended in 100 μ L of RIP Wash Buffer, followed by incubation with the addition of 5 μ g of antibodies according to the grouping for binding. Subsequently, the magnetic bead-antibody complex was resuspended in 900 μ L of RIP Wash Buffer after washing and then incubated overnight with 100 μ L of cell extract at 4 °C. Thereafter, the samples were placed on a magnetic pedestal to collect bead-protein complexes. The samples and input were detached by protease K, after which the RNA was extracted and used for subsequent RT-qPCR detection. The antibodies used in the experiment included rabbit monoclonal antibody against Ago2 (ab186733, 1:50, Abcam), which was mixed evenly at room temperature for 30 min. Rabbit anti-human IgG (ab109489, 1:100, Abcam) was used as an NC.

Cell counting kit-8 (CCK-8) assay

A CCK-8 kit (CA1210-100, Beijing Solarbio Science & Technology Co., Ltd.) was used in the experiment. Cells in logarithmic growth phase were inoculated into 96-well plates at a density of 5×10^3 cells/well and cultured for 3 days. Detection was conducted at 6 h after inoculation. Briefly, 10 μ L of CCK-8 solution was added to each well with the avoidance of bubbles in the wells, and the culture plate was placed in an incubator for a 2 h incubation. Subsequently, the optical density values at 450 nm were determined by a microplate reader (Model 680; Bio-Rad Laboratories, Hercules, CA, USA).

Transwell assay

A packing box containing a Transwell chamber (Millipore) was heated and placed in 24-well plates. The medium was placed in an incubator and preheated. Next, 0.5 mL of medium was added to the apical chamber supplemented with serum-free DMEM and basolateral chamber supplemented with DMEM containing 20% FBS, followed by 2 h of hydration and subsequent removal of the solution in the apical and basolateral chambers. After detachment, the cells were made into a cell suspension at a density of 5×10^4 cells/mL. Next, 0.5 mL of complete medium was added to the cells, and the hydration chambers were transferred to 24-well plates. Then, 0.1 mL of diluted cell suspension was added and incubated for 24 h, after which the liquid in the chambers was discarded. The cells in the membrane of the apical chamber were gently wiped with cotton, washed three times with PBS, fixed with precooled polyformaldehyde for 30 min,

stained with 1% crystal violet for 10 min, and then rinsed under running water. Finally, the dried crystal violet was observed under an inverted microscope (Olympus Optical Co., Ltd., Tokyo, Japan).

In the cell invasion experiments, the equipment used and experimental steps were consistent with those of the migration experiment. In addition, Matrigel (BD Biosciences, San Jose, CA, USA) was prepared and mixed well with DMEM at a ratio of 1:5. Next, 300 μ L of the mixture was added to the apical chamber and then incubated for 6 h. The appearance of the white layer indicated completion of Matrigel settlement. Prior to the experiment, the surface of the Matrigel was gently cleaned twice with PBS. The remaining steps were consistent with the cell migration experiment.

Flow cytometric analysis

After a 48 h period of transfection, the cells were detached using 0.25% trypsin without ethylenediaminetetraacetic acid and collected into flow tubes, followed by centrifugation and supernatant removal. Next, the cells were washed three times with cold PBS and centrifuged, and the supernatant was discarded. According to the Annexin-V-Fluorescein Isothiocyanate (FITC) cell apoptosis detection kit (556547, Shanghai Shuoji Biotechnology Co., Ltd., Shanghai, China), Annexin-V-FITC, propidium iodide (PI), and 4-(2-hydroxyethyl) piperazine-1-erhanesulfonic acid (HEPES) buffer solutions were prepared in Annexin-V/PI dye solutions at a ratio of 1:2:50. A total of 100 μ L of dye solution was used to suspend 1×10^6 cells, which were then mixed evenly with shaking. After incubation at room temperature for 15 min, 1 mL of HEPES buffer was added to the cells and mixed well with shaking. Afterward, cell apoptosis was measured by flow cytometry (Bio-Rad ZE5, Bio-Rad Laboratories). Fluorescence was initiated by excitation at 488 nm (FITC) and 535 nm (PI) and was measured by emission filters at 525 nm (FITC) and 615 nm (PI).

NSCLC xenografts in nude mice

Thirty specific pathogen-free male nude mice (aged 4–6 weeks old and weighing 15–20 g) were purchased from Shanghai SLAC Laboratory Animal Co., Ltd. (Shanghai, China). The nude mice were randomly grouped into 3 groups, with 10 mice in each group. NCI-H1975 cells that were infected with lentivirus expressing sh-NC, sh-DLGAP1-AS1 and sh-DLGAP1-AS1 + pcDNA-DTL were cultured, and then stably infected cell lines were obtained. The cell culture medium was gently washed with PBS and treated with 0.25% trypsin, and the reaction was terminated with complete medium. The cells were then centrifuged, and the supernatant was collected. An appropriate amount of normal saline was added and gently dissociated into a single cell suspension, after which the cells were counted. Then, 2×10^6 cells were resuspended in 50 mL of normal saline and mixed with 50 μ L of Matrigel Matrix at a ratio of 1:1. The mixture was subsequently inoculated into the axilla of nude mice in each group. On the 7th, 14th, 21st and 28th days after inoculation, the growth of tumors was observed and recorded. The short diameter (a) and long diameter (b) of tumors were recorded with a Vernier caliper. The volume of tumors was calculated according to the formula $\pi(a^2b)/6$. After the experiment, the nude mice were euthanized by cervical dislocation, and the tumors were extracted and photographed. Finally, the tumor was weighed. Western blot analysis was subsequently performed with the aim of detecting the protein expression of DTL in tumor tissues.

Statistical analysis

SPSS 21.0 software (IBM Corp., Armonk, NY, USA) was used for statistical data analyses. The measurement data are presented as the mean \pm standard deviation. Data obeying a normal distribution and homogeneity of variance between two groups were compared using paired *t*-tests, while those with defect variances were compared using unpaired *t*-tests. Data among multiple groups were assessed by one-way analysis of variance (ANOVA), followed by a Tukey multiple comparisons posttest. Statistical analysis in relation to time-based measurements within each group was realized using ANOVA of repeated measurements, followed by a Bonferroni multiple comparisons posttest. *p* < 0.05 was considered to be statistically significant.

RESULTS

lncRNA DLGAP1-AS1 is highly expressed in NSCLC tissues and cells

Prior studies have shown that lncRNA DLGAP1-AS1 serves as an oncogene in cancer, whereas its expression and mechanism of

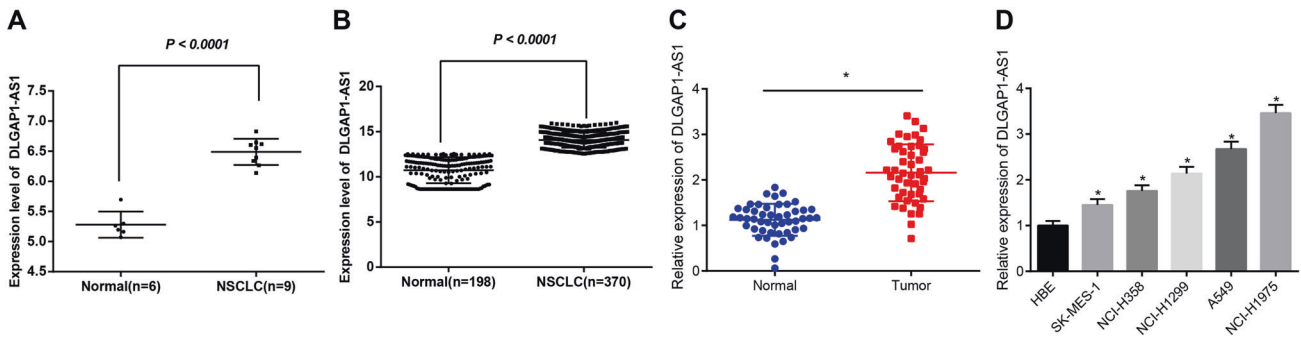


Fig. 1 Upregulated lncRNA DLGAP1-AS1 is found in NSCLC tissues and cells. **A** The expression of lncRNA DLGAP1-AS1 in microarray dataset GSE50627. **B** The expression of lncRNA DLGAP1-AS1 in microarray dataset GSE143018. **C** The expression of lncRNA DLGAP1-AS1 in NSCLC tissues and adjacent normal tissues determined by RT-qPCR ($n = 48$). **D** The expression of lncRNA DLGAP1-AS1 in A549, NCI-H1975, NCI-H1299, NCI-H358, SK-MES-1 and human bronchial epithelial cells determined by RT-qPCR; $*p < 0.05$, vs. adjacent normal tissues or HBE cell lines. Values are expressed as the mean \pm standard deviation; data between two groups were compared with paired t -test, and data among multiple groups were compared with one-way ANOVA, followed by a Tukey multiple comparisons posttest; the experiment was repeated 3 independent times.

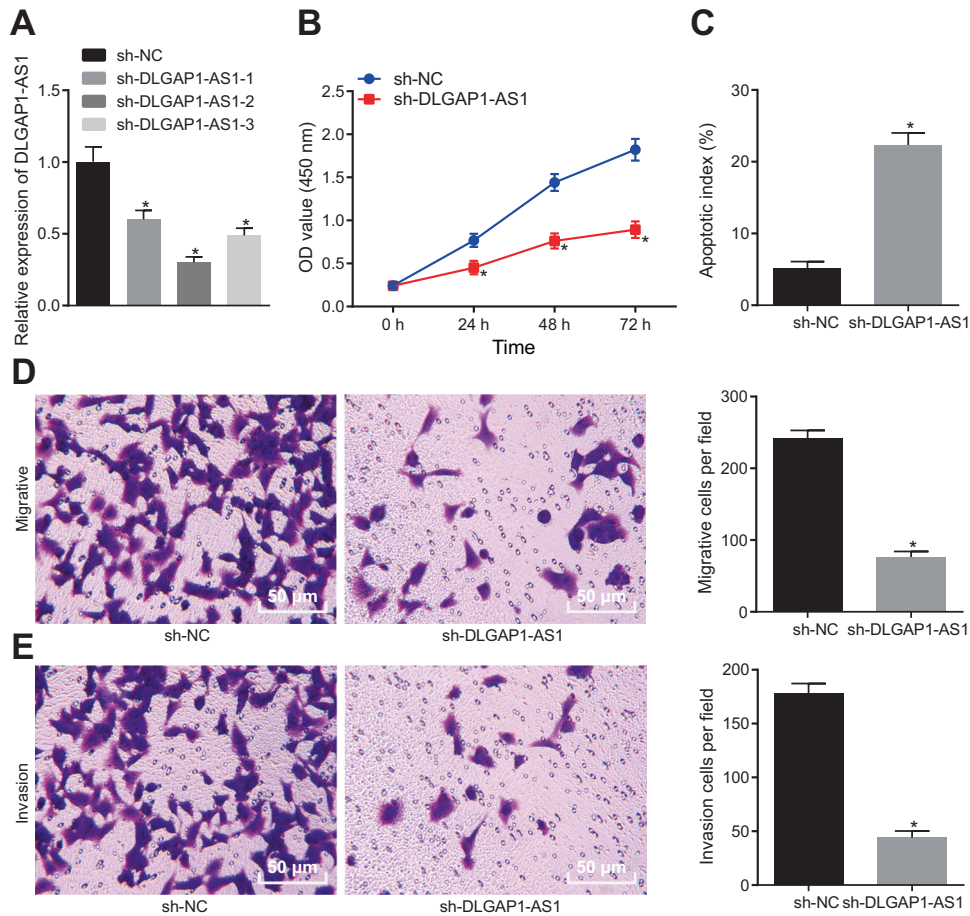


Fig. 2 Silencing of lncRNA DLGAP1-AS1 restricts NCI-H1975 cell viability, migration, and invasion but induces apoptosis in NCI-H1975 cells. **A** The expression of lncRNA DLGAP1-AS1 in NCI-H1975 cells determined by RT-qPCR. **B** The viability of NCI-H1975 cells assessed by CCK-8 assay. **C** The apoptosis of NCI-H1975 cells measured by flow cytometry. **D** The NCI-H1975 cell migration measured by Transwell assay ($\times 200$, scale bar = $50 \mu\text{m}$); $*p < 0.05$, vs. NCI-H1975 cells transfected with sh-NC; Values were expressed as the mean \pm standard deviation; data between two groups were compared with unpaired t -test and data among multiple groups were compared with one-way ANOVA, followed by a Tukey multiple comparisons posttest; Values of cell viability were analyzed using ANOVA of repeated measurements, followed by a Bonferroni post hoc test for multiple comparisons; the experiment was repeated 3 independent times.

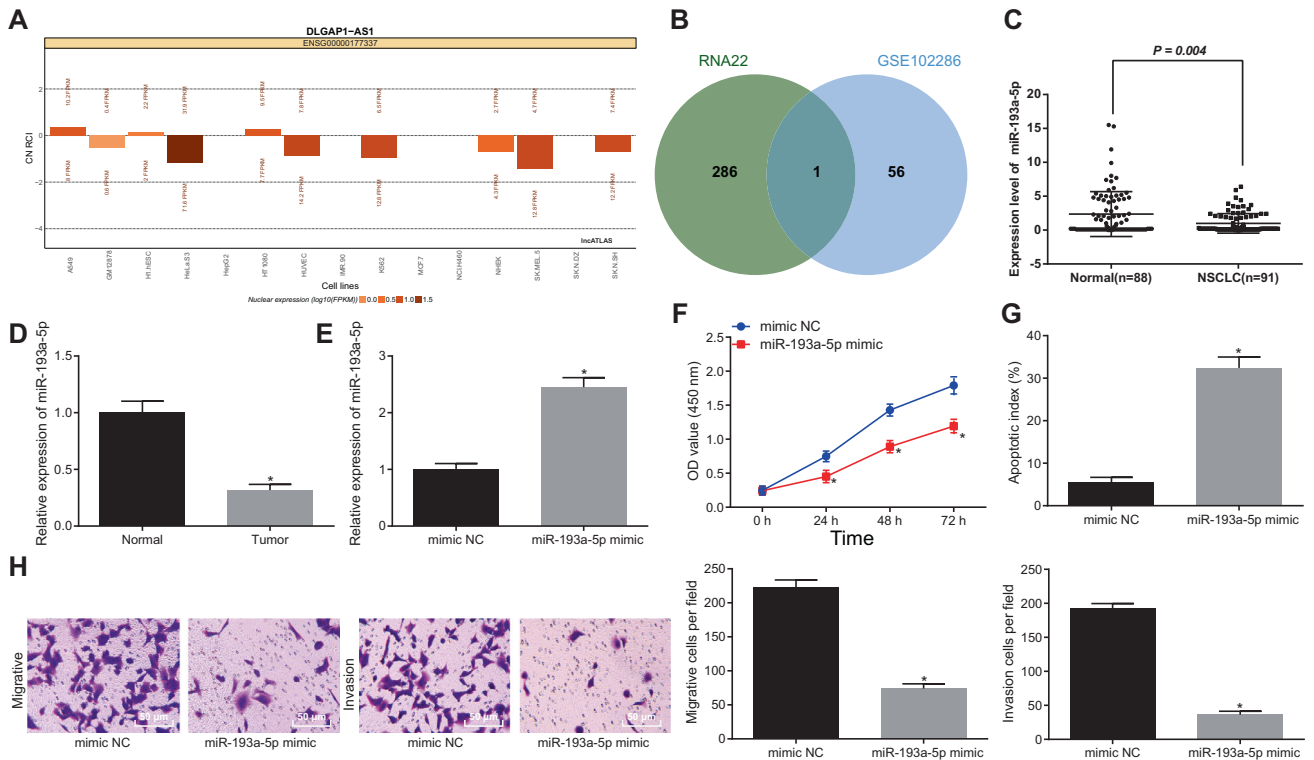


Fig. 3 Elevated expression of miR-193a-5p suppresses NSCLC cell viability, migration, and invasion, but induces apoptosis. **A** The localization of lncRNA DLGAP1-AS1 in NSCLC cells predicted with the LncAtlas database. **B** The Venn diagram displaying the intersection of putative miRNAs that might bind to lncRNA DLGAP1-AS1 predicted by RNA22 and differentially expressed miRNAs from the microarray dataset GSE102286. **C** The expression of miR-193a-5p in NSCLC tissues from the microarray dataset GSE102286. **D** The expression of miR-193a-5p in NSCLC and adjacent normal tissues determined by RT-qPCR, $n = 48$. **E** The expression of miR-193a-5p in NCI-H1975 cells determined by RT-qPCR. **F** The viability of NCI-H1975 cells assessed by CCK-8 assay. **G** The apoptosis of NCI-H1975 cells measured by flow cytometry. **H** The NCI-H1975 cell migration and invasion measured by Transwell assay ($\times 200$, scale bar = 50 μm); $*p < 0.05$, vs. adjacent normal tissues or NCI-H1975 cells transfected with mimic NC; $**p < 0.01$; Values were expressed as the mean \pm standard deviation and analyzed with paired t -test or unpaired t -test. Values of cell viability were analyzed using ANOVA of repeated measurements, followed by a Bonferroni post hoc test for multiple comparisons; the experiment was repeated 3 independent times.

action in NSCLC remain enigmatic^{11,16,17}. The expression of lncRNA DLGAP1-AS1 in NSCLC was analyzed in datasets GSE50627 and GSE143018 from GEO (Fig. 1A, B). It was found that lncRNA DLGAP1-AS1 was more highly expressed in NSCLC samples than in normal samples. As shown in Fig. 1C, the expression of lncRNA DLGAP1-AS1 in clinical NSCLC tissues was higher than that in adjacent normal tissues, as determined by RT-qPCR.

Then, we selected 5 NSCLC cell lines, A549, NCI-H1975, NCI-H1299, NCI-H358 and SK-MES-1, and human bronchial epithelial cells (HBE) for lncRNA DLGAP1-AS1 expression quantification by RT-qPCR. The results in Fig. 1D revealed that the expression of lncRNA DLGAP1-AS1 in NSCLC cells was higher than that in HBE cells. Furthermore, lncRNA DLGAP1-AS1 exhibited the highest expression in NCI-H1975 and A549 cells; therefore, NCI-H1975 and A549 cells were selected for subsequent experiments. In conclusion, lncRNA DLGAP1-AS1 was highly expressed in NSCLC tissues and cells.

Silencing of lncRNA DLGAP1-AS1 impedes NSCLC cell migration and invasion and contributes to apoptosis

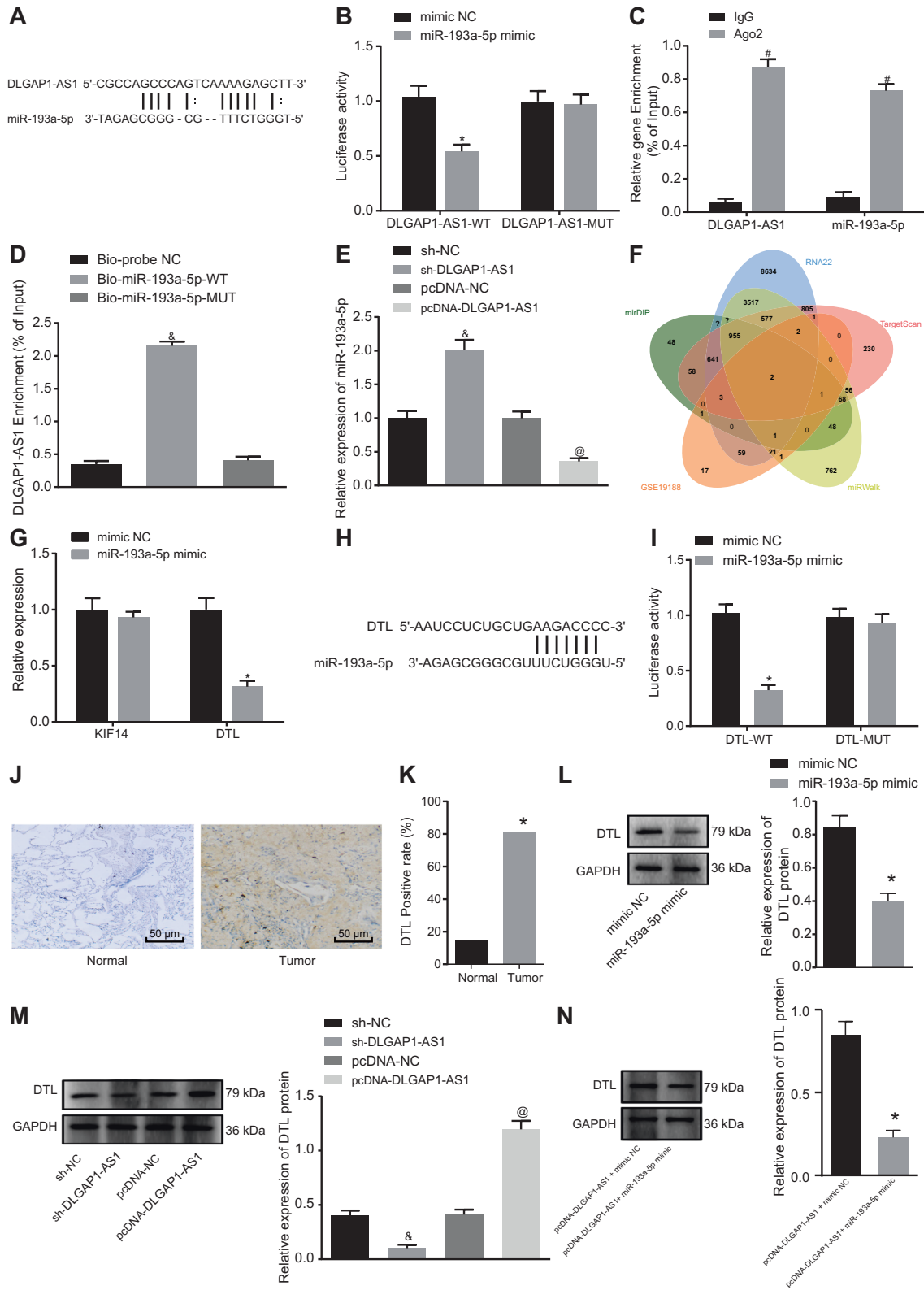
Three different lncRNA DLGAP1-AS1-specific shRNAs, sh-DLGAP1-AS1-1, sh-DLGAP1-AS1-2, and sh-DLGAP1-AS1-3, were developed to explore the function of lncRNA DLGAP1-AS1 in NSCLC. As depicted in Fig. 2A and Fig. S1A, the expression of lncRNA DLGAP1-AS1 in the presence of sh-DLGAP1-AS1-2 was decreased to the greatest degree. Therefore, sh-DLGAP1-AS1-2 was selected for further study. The results of the CCK-8 assay showed loss of viability in DLGAP1-AS1-depleted NCI-H1975 and A549 cells ($p < 0.01$) (Fig. 2B, Fig. S1B). Subsequent flow cytometry data revealed that the apoptotic rate of

NCI-H1975 and A549 cells transfected with sh-DLGAP1-AS1 was increased ($p < 0.01$) (Fig. 2C, Fig. S1C). Transwell assay results showed that the migration and invasion of NCI-H1975 and A549 cells transfected with sh-DLGAP1-AS1 were inhibited ($p < 0.01$) (Fig. 2D, E, Fig. S1D, E). Taken together, inhibition of lncRNA DLGAP1-AS1 exerted an inhibitory effect on the proliferation, migration and invasion of NSCLC cells while promoting apoptosis.

Overexpressed miR-193a-5p inhibits NSCLC cell viability, migration, and invasion but contributes to apoptosis

With the aforementioned results demonstrating the functional role of silencing lncRNA DLGAP1-AS1 in NSCLC, the location of lncRNA DLGAP1-AS1 in NSCLC cells was predicted by the LncAtlas database to investigate the downstream regulatory mechanism, which revealed that lncRNA DLGAP1-AS1 was mainly localized in the cytoplasm (Fig. 3A). It has been shown that cytoplasmic lncRNAs can competitively bind to miRNAs to regulate their expression¹⁸. To explore the regulatory mechanism of lncRNA DLGAP1-AS1 in NSCLC, we adopted the RNA22 database (<https://cm.jefferson.edu/rna22/>) for prediction, the results of which revealed 287 miRNAs possibly binding to lncRNA DLGAP1-AS1. The results were then intersected with 94 differentially expressed miRNAs from the NSCLC-related microarray dataset GSE102286 (p Value < 0.05 and $|\text{LogFoldChange}| > 1$), while hsa-miR-193a-5p was identified (Fig. 3B) and found to be significantly poorly expressed in NSCLC (Fig. 3C).

The results in Fig. 3D displayed much lower expression of miR-193a-5p in NSCLC tissues than in adjacent normal tissues, as



determined by RT-qPCR. RT-qPCR further demonstrated elevated expression of miR-193a-5p in NCI-H1975 cells treated with the miR-193a-5p mimic, suggesting successful overexpression efficiency (Fig. 3E). Afterward, the results obtained from the CCK-8 assay (Fig. 3F), flow cytometry (Fig. 3G), and Transwell assay (Fig. 3H) showed that the viability of NCI-H1975 cells transfected

with miR-193a-5p mimic was inhibited, the apoptotic rate was increased and migration and invasion were suppressed ($p < 0.05$). To conclude, these experimental data shed light on the suppressive action of overexpressed miR-193a-5p on NSCLC cell viability, migration and invasion accompanied by a promoting effect on apoptosis.

Fig. 4 LncRNA DLGAP1-AS1 upregulates DTL by binding to miR-193a-5p. **A** The binding site between miR-193a-5p and lncRNA DLGAP1-AS1. **B** The targeting relationship between lncRNA DLGAP1-AS1 and miR-193a-5p determined with dual luciferase reporter gene assay. **C** The enrichment of lncRNA DLGAP1-AS1 and miR-193a-5p assayed using RIP. **D** The enrichment of miR-193a-5p on DLGAP1-AS1 assessed with RNA pull-down. **E** The relative expression of miR-193a-5p in NSCLC cells determined with RT-qPCR. **F** The Venn diagram displaying the intersection of target genes of miR-193a-5p predicted by mirDIP, DIANA, RNA22, TargetScan and miRWalk and highly expressed genes from microarray dataset GSE19188. **G** The relative expression of KIF14 and DTL after miR-193a-5p expression was intervened in NSCLC cells determined with RT-qPCR. **H** The binding site between miR-193a-5p and DTL predicted with TargetScan. **I** The binding of miR-193a-5p to DTL confirmed by dual luciferase reporter gene assay. **J** The localization of DTL protein in NSCLC tissues and adjacent normal tissues detected by immunohistochemistry ($\times 200$, scale bar = 50 μm). **K** The positive expression of DTL protein in NSCLC tissues and adjacent normal tissues determined by immunohistochemistry, $n = 48$. **L** Western blot analysis for the protein expression level of DTL in presence of miR-193a-5p mimic. **M** Western blot analysis for the protein expression level of DTL in presence of sh-DLGAP1-AS1. **N** Western blot analysis for the protein expression level of DTL in presence of pcDNA-DLGAP1-AS1 + miR-193a-5p mimic; * $p < 0.05$, vs. adjacent normal tissues or NCI-H1975 cells transfected with mimic NC; # $p < 0.05$, vs. the IgG group; @ $p < 0.05$, vs. NCI-H1975 cells transfected with Bio-probe NC or sh-NC; @ $p < 0.05$, vs. NCI-H1975 cells transfected with pcDNA-NC; Values were expressed as the mean \pm standard deviation; data between two groups were compared with unpaired *t*-test and data among multiple groups were compared with one-way ANOVA, followed by a Tukey multiple comparisons posttest; the experiment was repeated 3 independent times.

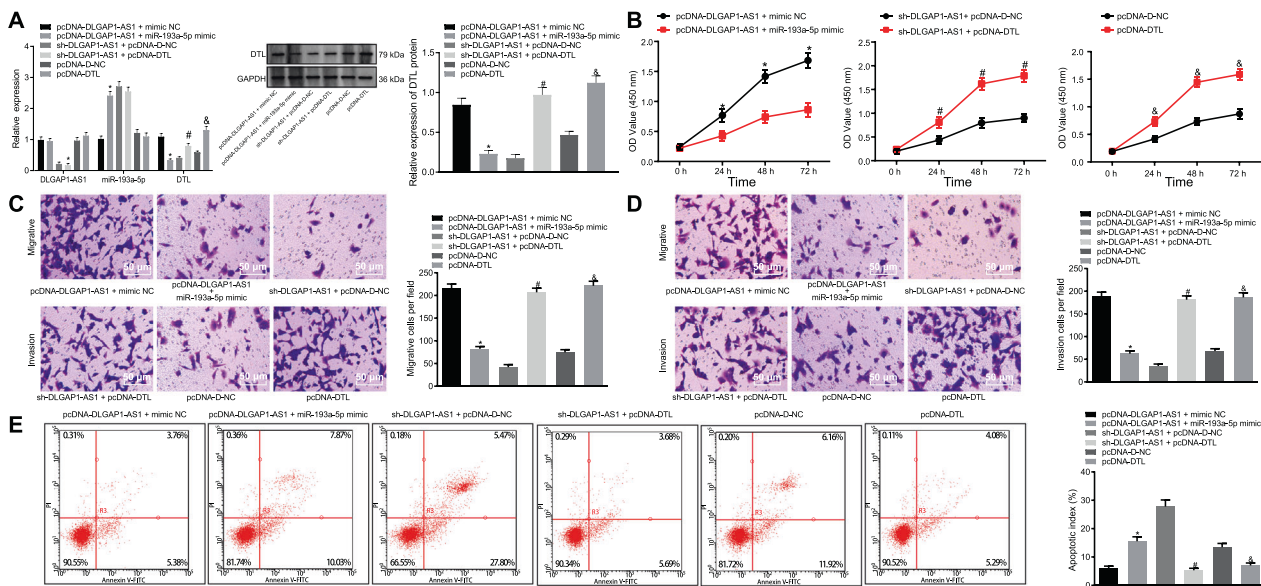


Fig. 5 Silencing lncRNA DLGAP1-AS1 suppresses NSCLC cell viability, migration, and invasion, but accelerates apoptosis via the miR-193a-5p/DTL axis. **A** The expression of lncRNA DLGAP1-AS1, miR-193a-5p and DTL determined by RT-qPCR and Western blot analysis. **B** The viability of cells assessed by CCK-8 assay. **C** The cell migration measured by Transwell assay ($\times 200$, scale bar = 50 μm). **D** The cell invasion measured by Transwell assay ($\times 200$, scale bar = 50 μm). **E** The cell apoptosis measured by flow cytometry; * $p < 0.05$, vs. NCI-H1975 cells transfected with pcDNA-DLGAP1-AS1 + mimic NC; # $p < 0.05$, vs. NCI-H1975 cells transfected with sh-DLGAP1-AS1 + pcDNA-D-NC; @ $p < 0.05$, vs. NCI-H1975 cells transfected with pcDNA-D-NC; Values were expressed as the mean \pm standard deviation; data among multiple groups were compared with one-way ANOVA, followed by a Tukey multiple comparisons posttest; Values of cell viability were analyzed using ANOVA of repeated measurements, followed by a Bonferroni post hoc test for multiple comparisons; the experiment was repeated 3 independent times.

LncRNA DLGAP1-AS1 binds to miR-193a-5p and elevates DTL expression

miR-193a-5p was predicted to bind to lncRNA DLGAP1-AS1 by bioinformatics analysis, and functional assays demonstrated the effect of overexpressed miR-193a-5p in NSCLC cells. Subsequent experiments were performed to detect the targeting relationship between lncRNA DLGAP1-AS1 and miR-193a-5p. The binding site between lncRNA DLGAP1-AS1 and miR-193a-5p was predicted on the RNA22 website (Fig. 4A). A dual luciferase reporter gene assay was then conducted for verification purposes. The results then conducted for verification the luciferase activity of DLGAP1-ASA-Wt in the presence of the miR-193a-5p mimic was significantly reduced, while the luciferase activity of DLGAP1-ASA-Mut was not significantly different (Fig. 4B). Next, a RIP assay was performed to further detect the relationship among lncRNA DLGAP1-AS1, miR-193a-5p and Ago2. The results showed that the enrichment of lncRNA DLGAP1-AS1 and miR-193a-5p in the Ago2 group was increased compared with that in the IgG group ($p < 0.05$) (Fig. 4C). Subsequent RNA pull-down experimental results verified that

lncRNA DLGAP1-AS1 enrichment was significantly elevated in the Bio-miR-193a-5p-Wt group but did not differ significantly in the Bio-miR-193a-5p-Mut group (all $p < 0.05$) (Fig. 4D). As reflected by RT-qPCR, silencing lncRNA DLGAP1-AS1 promoted the expression of miR-193a-5p, while the opposite trend was observed upon overexpression of lncRNA DLGAP1-AS1 (Fig. 4E). The above results indicate that lncRNA DLGAP1-AS1 could bind to miR-193a-5p.

Through mirDIP, RNA22, TargetScan, and miRWalk, the putative target genes of miR-193a-5p were intersected with 109 genes that were highly expressed in NSCLC screened from the NSCLC-related dataset GSE19188 (p -value < 0.05 and $|\text{LogFoldChange}| > 2$), revealing KIF14 and DTL (Fig. 4F). RT-qPCR results showed that overexpression of miR-193a-5p inhibited DTL expression ($p < 0.05$) but had no effect on KIF14 expression, so we chose DTL as the study subject for the subsequent analysis (Fig. 4G).

Next, the targeting binding site between miR-193a-5p and DTL was predicted with TargetScan (Fig. 4H). Meanwhile, the results from the dual luciferase reporter assay showed that miR-193a-5p mimic transfection resulted in decreased luciferase activity of Wt-DTL

($p < 0.05$), while no difference was detected in relation to the luciferase activity of Mut-DTL ($p > 0.05$), suggesting that miR-193a-5p may specifically bind to the DTL 3'UTR (Fig. 4I). In addition, immunohistochemistry was conducted to detect the expression and localization of DTL protein in NSCLC tissues, the results obtained from which indicated that DTL presented with yellow brown to brown granules in the cytoplasm (Fig. 4J), suggesting that DTL was mainly expressed in the cytoplasm. In comparison to adjacent normal tissues, DTL protein expression was evidently increased in NSCLC tissues [81.25% (39/48)] (Fig. 4K) (all $p < 0.05$). Western blot analysis results showed that overexpression of miR-193a-5p inhibited DTL protein expression (Fig. 4L). The aforementioned results encouraged us to conclude that DTL was highly expressed in NSCLC and that miR-193a-5p may target DTL and regulate its expression.

To verify the hypothesis that lncRNA DLGAP1-AS1 regulates DTL expression by binding to miR-193a-5p, we measured DTL expression after silencing lncRNA DLGAP1-AS1. Western blot analysis revealed an obviously decreased expression of DTL protein in the absence of DLGAP1-AS1 and an elevation of DTL protein in the presence of pcDNA-DLGAP1-AS1 (all $p < 0.05$) (Fig. 4M). DTL expression was further determined following alteration of lncRNA DLGAP1-AS1 and miR-193a-5p. Western blot analysis results showed that the transfection of miR-193a-5p mimic inhibited the effects of lncRNA DLGAP1-AS1 overexpression on DTL expression (Fig. 4N). Taken together, these findings provide evidence suggesting that lncRNA DLGAP1-AS1 can bind to miR-193a-5p and consequently reduce its expression to elevate DTL expression in NSCLC cells.

lncRNA DLGAP1-AS1 promotes NSCLC cell viability, migration, and invasion while inhibiting apoptosis via the miR-193a-5p/DTL axis

In an attempt to further dissect out the effects of lncRNA DLGAP1-AS1 on the migration, invasion, viability and apoptosis of NSCLC cells were dependent on miR-193a-5p and DTL, cells were transfected with sh-DLGAP1-AS1 + pcDNA-DTL, pcDNA-DLGAP1-

AS1 + miR-193a-5p mimic, and pcDNA-DTL. RT-qPCR and Western blot analysis revealed upregulated miR-193a-5p and downregulated DTL in the presence of pcDNA-DLGAP1-AS1 + miR-193a-5p mimic, yet lncRNA DLGAP1-AS1 expression did not differ significantly compared with pcDNA-DLGAP1-AS1 + mimic NC (Fig. 5A). When sh-DLGAP1-AS1 + pcDNA-DTL was delivered, DTL expression was significantly increased, without a significant difference detected regarding the expression of lncRNA DLGAP1-AS1 or miR-193a-5p. Compared with cells treated with pcDNA-D-NC, cells treated with pcDNA-DTL, sh-DLGAP1-AS1 + pcDNA-DTL or DLGAP1-AS1 exhibited upregulation of DTL, while miR-193a-5p expression was not significantly different.

Then, CCK-8 assays (Fig. 5B), Transwell assays (Fig. 5C, D) and flow cytometry (Fig. 5E) revealed that the viability, migration, and invasion of cells transfected with pcDNA-DLGAP1-AS1 + miR-193a-5p mimic were decreased, and cell apoptosis was increased. Moreover, sh-DLGAP1-AS1 + pcDNA-DTL treatment resulted in enhanced viability, migration, and invasion, along with a clear decline in relation to the apoptosis of NSCLC cells. Furthermore, compared with pcDNA-D-NC, pcDNA-DTL treatment resulted in enhanced viability, migration, and invasion but reduced apoptosis of NSCLC cells.

Altogether, lncRNA DLGAP1-AS1 promotes the viability, migration, and invasion of NSCLC cells and inhibits cell apoptosis via the miR-193a-5p/DTL axis.

Silencing lncRNA DLGAP1-AS1 retarded NSCLC tumor growth via the miR-193a-5p/DTL axis in vivo

The effects of lncRNA DLGAP1-AS1 and DTL on transplanted tumors in nude mice were tested in vivo based on the abovementioned in vitro results. Stable cells infected with lentivirus expressing sh-DLGAP1-AS1 and sh-DLGAP1-AS1 + pcDNA-DTL were injected into nude mice to construct subcutaneously transplanted tumor models. As shown in Fig. 6A–C, the tumor volume and weight of nude mice injected with cells infected with lentivirus expressing sh-DLGAP1-AS1 decreased

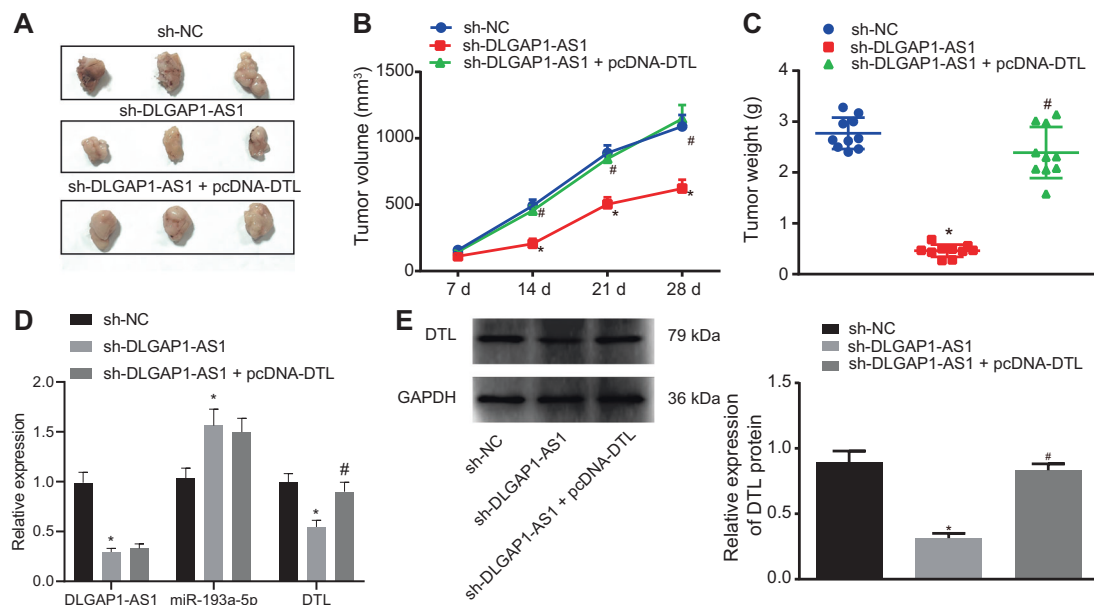


Fig. 6 Silencing of lncRNA DLGAP1-AS1 inhibits NSCLC tumor growth in vivo via the miR-193a-5p/DTL axis. **A** Representative images of tumors resected from nude mice. **B** Tumor volume. **C** Tumor weight. **D** Relative expression of lncRNA DLGAP1-AS1, miR-193a-5p and DTL determined by RT-qPCR. **E** Relative protein expression of DTL determined by Western blot analysis; * $p < 0.05$, vs. nude mice harboring NCI-H1975 cells transfected with sh-NC; # $p < 0.05$, vs. nude mice harboring NCI-H1975 cells transfected with sh-DLGAP1-AS1; $n = 10$; Values were expressed as the mean \pm standard deviation; data among multiple groups were compared with one-way ANOVA, followed by a Tukey multiple comparisons posttest; Values of cell viability were analyzed using ANOVA of repeated measurements, followed by a Bonferroni post hoc test for multiple comparisons; the experiment was repeated 3 independent times.

($p < 0.05$). In addition, the tumor volume and weight of nude mice injected with cells infected with lentivirus expressing sh-DLGAP1-AS1 + pcDNA-DTL increased remarkably ($p < 0.05$). Furthermore, Western blot analysis and RT-qPCR showed that DTL and DLGAP1-AS1 expression was decreased, and miR-193a-5p expression was enhanced in tumor tissues in response to infection with lentivirus expressing sh-DLGAP1-AS1 ($p < 0.05$); however, the expression of DTL was elevated in NSCLC tissues in response to infection with lentivirus expressing sh-DLGAP1-AS1 + pcDNA-DTL, but DLGAP1-AS1 and miR-193a-5p expression showed no significant difference ($p < 0.05$) (Fig. 6D, E).

Altogether, knockdown of lncRNA DLGAP1-AS1 prevents the growth of tumors in mice with NSCLC via the miR-193a-5p/DTL axis.

DISCUSSION

Lung cancer is one of the most malignant cancers worldwide, with the rapidest disease progression and the lowest survival rate¹⁹. It is necessary to take precautions to avoid lung cancers as well as develop accurate methods that can diagnose NSCLC at the early stage, which can raise the survival possibility of patients. Although one noninvasive method, low-dose computed tomography, has been explored to reduce mortality from lung cancer, it will also give a false-positive result, which may result in unnecessary treatments or suffering for certain patients²⁰. Under these conditions, noncoding RNAs exhibit two significant advantages as excellent biomarkers to diagnose NSCLC in the early stage. One is that both miRNAs and lncRNAs are relatively stable in blood, and their expression is tissue-specifically enriched in disease conditions²¹. This allows noncoding RNAs to be easily determined with minor samples. The other one is predictive indicators. Traditionally, taking coding genes as biomarkers always lags behind disease progression. Hence, the accumulated mutations that are already present in coding genes can only help diagnose disease instead of predicting disease. Noncoding RNAs usually act as upregulators to control downstream coding gene expression in epigenetic ways²¹. Once disease proceeds, alterations in noncoding RNAs are always found before coding genes. Hence, it is promising to develop noncoding RNA biomarkers as predictive indicators or as early diagnostic indicators. In this study, we found that both lncRNA DLGAP1-AS1 and DTL were highly expressed in NSCLC tissues and cells. lncRNA DLGAP1-AS1 regulated DTL expression by binding to miR-193a-5p. Inhibition of either lncRNA DLGAP1-AS1 or DTL suppressed viability, migration, and invasion and promoted apoptosis of NSCLC tumor cells both in vitro and in vivo.

Many other lncRNAs have also been identified as having oncogenic roles in NSCLC, such as lncRNA DLGAP1-AS1. For example, lncRNA colon cancer associated transcript 2 (CCAT2) is highly expressed in lung adenocarcinoma, and silencing lncRNA CCAT2 reduces viability and metastasis in lung adenocarcinoma²². Likewise, increased expression of lncRNA plasmacytoma variant translocation 1 (PVT1) is found in NSCLC lung samples, while small interfering RNA against lncRNA PVT1 leads to inhibited cancer cell viability, migration, and invasion²³. Consistently, lncRNA DLGAP1-AS1 expression was elevated in gastric cancer tissue samples and cell lines, while its depletion suppressed the aggressive behavior of gastric cells, hindered tumor growth and enhanced cell apoptosis¹¹. It has been shown that lncRNA DLGAP1-AS1 plays an oncogenic role associated with advanced tumor progression of hepatocellular carcinoma and epithelial-mesenchymal transition¹⁶. These studies further supported our finding that lncRNA DLGAP1-AS1 also serves as a general oncogenic indicator in NSCLC.

In contrast, miR-193a-5p has been reported as an anti-oncogene in NSCLC. However, in contrast to our result that DTL was specifically targeted by miR-193a-5p, a previous study showed that the expression of miR-193a in lung cancer tissues was

reduced compared to that in adjacent nontumor tissues and that its elevation decreased the growth of tumor xenografts by targeting the WT1-E-cadherin axis⁸. These results suggested that miR-193a-5p might regulate NSCLC via diverse signaling pathways by targeting different genes. Additionally, other reports have also revealed the lncRNA/miRNA regulatory network that regulates NSCLC progression. For instance, lncRNA urothelial carcinoembryonic antigen 1 (UCA1) increases ERBB4 gene expression by binding to miR-193a-3p. Impaired expression of lncRNA UCA1 reduces the viability of NSCLC cells²⁴. Similarly, lncRNA nuclear paraspeckle assembly transcript 1 regulates hsa-miR-377-3p, which specifically targets E2F transcription factor 3 in NSCLC progression²⁵. Moreover, highly expressed DTL was revealed to be engaged in the dismal prognosis of patients with multiple cancers, including lung cancer²⁶. Likewise, the hsa_circ_0072305/hsa-miR-127-5p/DTL network was identified to serve as a biomarker for the occurrence and development of NSCLC²⁷. DTL is amplified in approximately 7% of NSCLC cases in relation to the disease recurrence of patients who have undergone surgical resection²⁸. Largely in agreement with our findings, highly expressed DTL has been reported in NSCLC tissues and cells, while miR-203 target inhibition of DTL harbors antineoplastic properties²⁹. Therefore, the lncRNA/miRNA/mRNA axis is a general regulatory pattern in NSCLC progression that can be applied for drug targets.

In conclusion, the lncRNA DLGAP1-AS1/miR-193a-5p/DTL axis regulated NSCLC progression in such a way that DLGAP1-AS1 upregulated DTL by binding to miR-193a-5p. Either inhibition of lncRNA DLGAP1-AS1 or DTL suppressed tumor development and promoted apoptosis both in vitro and in vivo. Hence, it is possible to develop biomarkers according to the lncRNA DLGAP1-AS1/miR-193a-5p/DTL axis. Furthermore, it is promising to explore drugs targeting lncRNA DLGAP1-AS1 or DTL genes to treat NSCLC in the future.

DATA AVAILABILITY

The datasets generated/analysed during the current study are available.

REFERENCES

- Siegel, RL, Miller, KD, Jemal, A. Cancer statistics, 2015. *CA Cancer J Clin* **65**, 5–29 (2015)
- Molina, JR, Yang, P, Cassivi, SD, Schild, SE, Adjei, AA. Non-small cell lung cancer: Epidemiology, risk factors, treatment, and survivorship. *Mayo Clin Proc* **83**, 584–594 (2008)
- Shigematsu, H, Gazdar, AF. Somatic mutations of epidermal growth factor receptor signaling pathway in lung cancers. *Int J Cancer* **118**, 257–262 (2006)
- Li, T, Kung, HJ, Mack, PC, Gandara, DR. Genotyping and genomic profiling of non-small-cell lung cancer: implications for current and future therapies. *J Clin Oncol* **31**, 1039–1049 (2013)
- Farazi, TA, Hoell, JI, Morozov, P, Tuschl, T. MicroRNAs in human cancer. *Adv Exp Med Biol* **774**, 1–20 (2013)
- Hu, Z, Chen, X, Zhao, Y, Tian, T, Jin, G, Shu, Y, et al. Serum microRNA signatures identified in a genome-wide serum microRNA expression profiling predict survival of non-small-cell lung cancer. *J Clin Oncol* **28**, 1721–1726 (2010)
- Kumar, MS, Erkeland, SJ, Pester, RE, Chen, CY, Ebert, MS, Sharp, PA, et al. Suppression of non-small cell lung tumor development by the let-7 microRNA family. *Proc Natl Acad Sci USA* **105**, 3903–3908 (2008)
- Chen, J, Gao, S, Wang, C, Wang, Z, Zhang, H, Huang, K, et al. Pathologically decreased expression of miR-193a contributes to metastasis by targeting WT1-E-cadherin axis in non-small cell lung cancers. *J Exp Clin Cancer Res* **35**, 173 (2016)
- Nakagawa, T, Endo, H, Yokoyama, M, Abe, J, Tamai, K, Tanaka, N, et al. Large noncoding RNA HOTAIR enhances aggressive biological behavior and is associated with short disease-free survival in human non-small cell lung cancer. *Biochem Biophys Res Commun* **436**, 319–324 (2013)
- Dong, Y, Liang, G, Yuan, B, Yang, C, Gao, R, Zhou, X. MALAT1 promotes the proliferation and metastasis of osteosarcoma cells by activating the PI3K/Akt pathway. *Tumour Biol* **36**, 1477–1486 (2015)
- Deng, J, Zhang, Q, Lu, L, Fan, C. Long Noncoding RNA DLGAP1-AS1 promotes the aggressive behavior of gastric cancer by acting as a ceRNA for microRNA-628-5p and raising astrocyte elevated gene 1 Expression. *Cancer Manag Res* **12**, 2947–2960 (2020)

12. Gautier, L, Cope, L, Bolstad, BM, Irizarry, RA. *affy*-analysis of Affymetrix GeneChip data at the probe level. *Bioinformatics* **20**, 307–315 (2004)
13. Smyth GK. Linear models and empirical bayes methods for assessing differential expression in microarray experiments. *Stat Appl Genet Mol Biol* **3**, Article3 (2004) <https://doi.org/10.2202/1544-6115.1027>. Epub 2004 Feb 12. PMID: 16646809.
14. Sun, Y, Li, D, Lv, XH, Hua, SC, Han, JC, Xu, F, et al. Roles of osteopontin and matrix metalloproteinase-7 in occurrence, progression, and prognosis of nonsmall cell lung cancer. *J Res Med Sci* **20**, 1138–1146 (2015)
15. Feng, J, Sun, Y, Zhang, EB, Lu, XY, Jin, SD, Guo, RH. A novel long noncoding RNA IRAIN regulates cell proliferation in non small cell lung cancer. *Int J Clin Exp Pathol* **8**, 12268–12275 (2015)
16. Lin, Y, Jian, Z, Jin, H, Wei, X, Zou, X, Guan, R, et al. Long non-coding RNA DLGAP1-AS1 facilitates tumorigenesis and epithelial-mesenchymal transition in hepatocellular carcinoma via the feedback loop of miR-26a/b-5p/IL-6/JAK2/STAT3 and Wnt/beta-catenin pathway. *Cell Death Dis* **11**, 34 (2020)
17. Peng, X, Wei, F, Hu, X. Long noncoding RNA DLGAP1-AS1 promotes cell proliferation in hepatocellular carcinoma via sequestering miR-486-5p. *J Cell Biochem* **121**, 1953–1962 (2020)
18. Salmena, L, Poliseno, L, Tay, Y, Kats, L, Pandolfi, PP. A ceRNA hypothesis: The Rosetta Stone of a hidden RNA language? *Cell* **146**, 353–358 (2011)
19. Lv, J, Qiu, M, Xia, W, Liu, C, Xu, Y, Wang, J, et al. High expression of long non-coding RNA SBF2-AS1 promotes proliferation in non-small cell lung cancer. *J Exp Clin Cancer Res* **35**, 75 (2016)
20. National Lung Screening Trial Research, T, Aberle, DR, Adams, AM, Berg, CD, Black, WC, Clapp, JD, et al. Reduced lung-cancer mortality with low-dose computed tomographic screening. *N Engl J Med* **365**, 395–409 (2011)
21. Ricciuti, B, Mencaroni, C, Paglialonga, L, Paciullo, F, Crino, L, Chiari, R, et al. Long noncoding RNAs: new insights into non-small cell lung cancer biology, diagnosis and therapy. *Med Oncol* **33**, 18 (2016)
22. Qiu, M, Xu, Y, Yang, X, Wang, J, Hu, J, Xu, L, et al. CCAT2 is a lung adenocarcinoma-specific long non-coding RNA and promotes invasion of non-small cell lung cancer. *Tumour Biol* **35**, 5375–5380 (2014)
23. Yang, YR, Zang, SZ, Zhong, CL, Li, YX, Zhao, SS, Feng, XJ. Increased expression of the lncRNA PVT1 promotes tumorigenesis in non-small cell lung cancer. *Int J Clin Exp Pathol* **7**, 6929–6935 (2014)
24. Nie, W, Ge, HJ, Yang, XQ, Sun, X, Huang, H, Tao, X, et al. LncRNA-UCA1 exerts oncogenic functions in non-small cell lung cancer by targeting miR-193a-3p. *Cancer Lett* **371**, 99–106 (2016)
25. Sun, C, Li, S, Zhang, F, Xi, Y, Wang, L, Bi, Y, et al. Long non-coding RNA NEAT1 promotes non-small cell lung cancer progression through regulation of miR-377-3p-E2F3 pathway. *Oncotarget* **7**, 51784–51814 (2016)
26. Xue, JM, Liu, Y, Wan, LH, Zhu, YX. Comprehensive analysis of differential gene expression to identify common gene signatures in multiple cancers. *Med Sci Monit* **26**, e919953 (2020)
27. Cai, X, Lin, L, Zhang, Q, Wu, W, Su, A. Bioinformatics analysis of the circRNA-miRNA-mRNA network for non-small cell lung cancer. *J Int Med Res* **48**, 300060520929167 (2020)
28. Perez-Pena, J, Corrales-Sanchez, V, Amir, E, Pandiella, A, Ocana, A. Ubiquitin-conjugating enzyme E2T (UBE2T) and denticleless protein homolog (DTL) are linked to poor outcome in breast and lung cancers. *Sci Rep* **7**, 17530 (2017)
29. Ma, T, Hu, Y, Guo, Y, Zhang, Q. Human umbilical vein endothelial cells-derived microRNA-203-containing extracellular vesicles alleviate non-small-cell lung cancer progression through modulating the DTL/p21 axis. *Cancer Gene Ther* Feb 8 (2021) <https://doi.org/10.1038/s41417-020-00292-3>

AUTHOR CONTRIBUTIONS

Xudong Pan conceived and designed research. Siwen Chen performed experiments and interpreted results of experiments. Lu Ye analyzed data. Shenjie Xu prepared figures. Ling Wang drafted paper. Yi Sun edited and revised manuscript. All authors read and approved final version of manuscript.

FUNDING

This work is supported by National Natural Science Foundation of China (No. 31101641) and the project Funded by the Priority Academic Program Development of Jiangsu Higher Education Institutions.

COMPETING INTERESTS

The authors declare no competing interests.

ETHICS APPROVAL AND CONSENT TO PARTICIPATE

The study was performed with the approval of the Ethics Committee of The First Affiliated Hospital of Soochow University. Each patient provided informed written consent prior to study recruitment. All experiments in the present study were conducted in strict accordance with the Helsinki Declaration. The animal experiment strictly adhered to the principle to minimize the pain, suffering, and discomfort to experimental animals. The protocol was approved by the Animal Ethics Committee of The First Affiliated Hospital of Soochow University.

ADDITIONAL INFORMATION

Supplementary information The online version contains supplementary material available at <https://doi.org/10.1038/s41374-022-00831-6>.

Correspondence and requests for materials should be addressed to Ling Wang or Yi Sun.

Reprints and permission information is available at <http://www.nature.com/reprints>

Publisher's note Springer Nature remains neutral with regard to jurisdictional claims in published maps and institutional affiliations.

Springer Nature or its licensor holds exclusive rights to this article under a publishing agreement with the author(s) or other rightsholder(s); author self-archiving of the accepted manuscript version of this article is solely governed by the terms of such publishing agreement and applicable law.